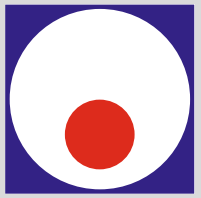




FACULTY OF MECHANICAL AND CIVIL ENGINEERING
IN KRALJEVO
UNIVERSITY OF KRAGUJEVAC



XI TRIENNIAL
INTERNATIONAL CONFERENCE
**HEAVY
MACHINERY
HM 2023**
Proceedings

VRNJAČKA BANJA, SERBIA
June 21– June 24, 2023



**FACULTY OF MECHANICAL AND CIVIL ENGINEERING IN KRALJEVO
UNIVERSITY OF KRAGUJEVAC
KRALJEVO – SERBIA**

THE ELEVENTH TRIENNIAL INTERNATIONAL CONFERENCE

HEAVY MACHINERY HM 2023

PROCEEDINGS

ORGANIZATION SUPPORTED BY:

Ministry of Science, Technological Development and Innovation, Republic of Serbia

Vrnjačka Banja, June 21–24, 2023



PUBLISHER:

Faculty of Mechanical and Civil Engineering in Kraljevo

YEAR:

2023

EDITOR:

Prof. dr Mile Savković

PRINTOUT:

SATCIP DOO VRNJAČKA BANJA

TECHNICAL COMMITTEE

Doc. dr Aleksandra Petrović – Chairman

Bojan Beloica – Vice-chairman

Miloš Adamović

Goran Bošković

Vladimir Đorđević

Marina Ivanović

Marijana Janićijević

Aleksandar Jovanović

Stefan Mihajlović

Predrag Mladenović

Stefan Pajović

Anica Pantić

Nevena Petrović

Mladen Rasinac

Vladimir Sinđelić

Marko Todorović

Đorđe Novčić

Jovana Bojković

Tanja Miodragović

Jovana Perić

Slobodan Bukarica

No. of copies: 60

ISBN-978-86-82434-01-6

REVIEWS:

All papers have been reviewed by members of scientific committee



CONFERENCE CHAIRMAN

Prof. dr Mile Savković, FMCE Kraljevo, Serbia

INTERNATIONAL SCIENTIFIC PROGRAM COMMITTEE

CHAIRMAN

Prof. dr Radovan Bulatović, FMCE Kraljevo, Serbia

VICE-CHAIRMAN

Prof. dr Milan Bižić, FMCE Kraljevo, Serbia

MEMBERS

Prof. dr M. Alamoreanu, TU Bucharest, Romania

Prof. dr D. Atmadzhova, VTU “Todor Kableskov”, Sofia, Bulgaria

Prof. dr M. Banić, FME Niš, Serbia

Prof. dr M. Berg, Royal Institute of Technology-KTH, Sweden

Prof. dr G. Bogdanović, Faculty of Engineering Kragujevac, Serbia

Prof. dr H. Bogdevicius, Technical University, Vilnius, Lithuania

Prof. dr N. Bogojević, FMCE Kraljevo, Serbia

Prof. dr I. Božić, FME Belgrade, Serbia

Prof. dr S. Bikić, Faculty of Technical Sciences, Novi Sad, Serbia

Prof. dr M. Bjelić, FMCE Kraljevo, Serbia

Prof. dr M. Blagojević, Faculty of Engineering Kragujevac, Serbia

Prof. dr S. Bošnjak, FME Belgrade, Serbia

Prof. dr A. Bruja, TU Bucharest, Romania

Prof. dr S. Ćirić-Kostić, FMCE Kraljevo, Serbia

Prof. dr I. Despotović, FMCE Kraljevo, Serbia

Prof. dr M. V. Dragoi, Transilvania University of Brasov, Romania

Prof. dr B. Dragović, Faculty of Maritime Studies Kotor, Montenegro

Prof. dr Lj. Dubonjić, FMCE Kraljevo, Serbia

Prof. dr R. Durković, FME Podgorica, Montenegro

Prof. dr Z. Đinović, ACMIT, Wiener Neustadt, Austria

Prof. dr R. Đokić, Faculty of Technical Sciences, Novi Sad, Serbia

Prof. dr K. Ehmann, Northwestern University, Chicago, USA

Prof. dr I. Emeljanova, HGTUSA Harkov, Ukraine

Prof. dr O. Erić Cekić, FMCE Kraljevo, Serbia

Prof. dr V. Gašić, FME Belgrade, Serbia

Prof. dr D. Golubović, FME East Sarajevo, Bosnia and Herzegovina

Prof. dr P. Gvero, FME Banja Luka, Bosnia and Herzegovina

Prof. dr B. Jerman, FME Ljubljana, Slovenia

Prof. dr R. Karamarković, FMCE Kraljevo, Serbia

Prof. dr M. Karasahin, Demirel University, Istanbul, Turkey

Prof. dr I. Kiričenko, HNADU Kiev, Ukraine

Prof. dr K. Kocman, Technical University of Brno, Czech Republic

Prof. dr S. Kolaković, Faculty of Technical Sciences, Novi Sad, Serbia

Prof. dr M. Kolarević, FMCE Kraljevo, Serbia

Prof. dr M. Kostić, Northern Illinois University, DeKalb, USA

Prof. dr M. Krajišnik, FME East Sarajevo, Bosnia and Herzegovina

Prof. dr M. Králik, FME Bratislava, Slovakia

Prof. dr E. Kudrjavcev, MGSU, Moscow, Russia

Prof. dr Đ. Lađinović, Faculty of Technical Sciences, Novi Sad, Serbia

Prof. dr D. Marinković, TU Berlin, Germany

Prof. dr G. Marković, FMCE Kraljevo, Serbia

Prof. dr A. Milašinović, FME Banja Luka, Bosnia and Herzegovina

Prof. dr I. Milićević, Technical Faculty Čačak, Serbia

Prof. dr V. Milićević, FMCE Kraljevo, Serbia

Prof. dr Z. Miljković, FME Belgrade, Serbia



Prof. dr D. Milković, FME Belgrade, Serbia
Prof. dr B. Milošević, FMCE Kraljevo, Serbia
Prof. dr V. Milovanović, Faculty of Engineering
Kragujevac, Serbia
Prof. dr G. Minak, University of Bologna, Italy
Prof. dr D. Minić, FME Kosovska Mitrovica,
Serbia
Prof. dr V. Nikolić, FME Niš, Serbia
Prof. dr E. Nikolov, Technical University, Sofia,
Bulgaria
Prof. dr V. Nikolov, VTU “Todor Kableshkov”,
Sofia, Bulgaria
Prof. dr M. Ognjanović, FME Belgrade, Serbia
Prof. dr J. Peterka, FMS&T, Trnava, Slovakia
Prof. dr D. Petrović, FMCE Kraljevo, Serbia
Prof. dr M. Popović, Technical Faculty Čačak,
Serbia
Prof. dr J. Polajnar, BC University, Prince
George, Canada
Prof. dr D. Pršić, FMCE Kraljevo, Serbia
Prof. dr N. Radić, FME East Sarajevo, Bosnia
and Herzegovina

Prof. dr B. Radičević, FMCE Kraljevo, Serbia
Prof. dr V. Radonjanin, Faculty of Technical
Sciences, Novi Sad, Serbia
Prof. dr D. Sever, Maribor, Civil Engineering,
Slovenia
Prof. dr V. Stojanović, FMCE Kraljevo, Serbia
Prof. dr I. S. Surovcev, VGSU, Voronezh,
Russia
Prof. dr S. Šalinić, FMCE Kraljevo, Serbia
Prof. dr J. Tanasković, FME Belgrade, Serbia
Prof. dr LJ. Tanović, FME Belgrade, Serbia
Prof. dr D. Todorova, VTU “Todor
Kableshkov”, Sofia, Bulgaria
Prof. dr R. Vujadinovic, FME Podgorica,
Montenegro
Prof. dr K. Weinert, University of Dortmund,
Germany
Prof. dr N. Zdravković, FMCE Kraljevo, Serbia
Prof. dr N. Zrnić, FME Belgrade, Serbia
Prof. dr D. Živanić, Faculty of Technical
Sciences, Novi Sad, Serbia

ORGANIZING COMMITTEE

CHAIRMAN:

Prof. dr Goran Marković, FMCE Kraljevo

VICE-CHAIRMAN:

Doc. dr Miljan Marašević, FMCE Kraljevo, Serbia

MEMBERS:

Doc. dr M. Bošković, FMCE Kraljevo, Serbia
Doc. dr V. Grković, FMCE Kraljevo, Serbia
Doc. dr V. Mandić, FMCE Kraljevo, Serbia
Doc. dr A. Nikolić, FMCE Kraljevo, Serbia
Doc. dr M. Nikolić, FMCE Kraljevo, Serbia

Doc. dr A. Petrović, FMCE Kraljevo, Serbia
Doc. dr B. Sredojević, FMCE Kraljevo, Serbia
Dr N. Pavlović, FMCE Kraljevo, Serbia
Doc. dr N. Stojić, FMCE Kraljevo, Serbia

Nonlinear static „pushover” analysis of multi-storey reinforced concrete building

Marijana Janićijević^{1*}, Bojan Milošević¹, Stefan Mihajlović¹, Jovana Bojković¹, Saša Marinković²

¹Faculty of Mechanical and Civil Engineering, University of Kragujevac, Kraljevo (Republic of Serbia)

²Marko Barlov PR izgradnja stambenih i nestambenih objekata LMT Inženjering Kraljevo

Contemporary structural design implies the nonlinear behaviour of ductile structural elements for the design of seismic actions, which implies the application of nonlinear analysis. Pushover analysis evaluates the seismic performance of the structure and combines the behavior of bearing and non-bearing elements thus forming a description of the overall degree of damage to the construction for different levels of seismic action.

This paper presents the results of the nonlinear static "pushover" analysis of a multi-storey reinforced concrete building designed according to EN 1992-1-1 and EN 1998-1. The structure was exposed to a monotonically increasing lateral load. The analysis was performed using four different material nonlinearity models (infrmFB, infrmDB, infrmFBPH, infrmDBPH) for two orthogonal directions in the SeismoStruct program. The assessment of seismic performance of the structure was performed based on the results of the "pushover" analysis for each of the applied nonlinear material models.

Keywords: pushover analysis, material nonlinearity, target displacement, seismic action

1. INTRODUCTION

The territory of the Republic of Serbia belongs to seismically active areas, so when designing and constructing buildings, it is necessary to apply regulations and methods that ensure seismic resistance. In this sense, it is necessary to use appropriate input data (depending on local conditions) and appropriate design and building methods. The objectives of seismic design are: to limit damage to structures, protect human life, and ensure the use of facilities that are important for emergency response in the event of earthquakes.

According to the modern seismic codes for the design of structures resistant to the effects of earthquakes, the concept of the design of reinforced concrete structures, in addition to ensuring strength capacity, is based on reducing the elastic seismic inertia effects while ensuring adequate ductility of the critical zones[1]. The structure doesn't need to remain elastic under the influence of the intended seismic loading. The development of inelastic deformations of the bearing elements is allowed to preserve the integrity of the entire structure. Based on the linear design approach, it is not possible to determine the nonlinear deformations that will occur due to the given seismic action, and therefore the extent of damage to the structure remains unknown [2]. A comprehensive design approach includes the non-linear behavior of structural elements during moderate and strong earthquakes, in pre-defined critical zones, which enables the dissipation of seismic energy. The energy dissipation capacity depends on the extent of the non-linear response of the structure. The main feature of the aseismic design is the use of behaviour factors, balancing strength, and ductility introduced through different classes of ductility. For dissipative structures, the value of the behavior factor is greater than 1.5, resulting in hysteretic energy dissipation in specific areas (critical zones). According to EN 1998-1, buildings can be classified into three different ductility classes depending on the degree of energy dissipation: low ductility class (*DCL*), medium ductility class (*DCM*), and high ductility class (*DCH*).

Modern seismic analysis is based on the determination of the dynamic properties of the structure, the determination of the seismic force based on the given ground displacement and the mechanical properties of the structure, and the calculation of the effects on the structure as a result of the action of the relevant seismic forces. After the aforementioned influences are determined, all elements and critical sections are dimensioned for the appropriate combination of all loads acting on the structure (including the seismic load). The bearing capacity and the required deformation capacity of the considered structure are achieved by applying appropriate structural solutions and by elaborating specific details according to the seismic design requirements.

2. NONLINEAR STATIC ANALYSIS

In aseismic design, pushover analysis can be used as an alternative to linear-elastic analysis. The pushover method is a non-linear static method of calculating new or existing objects. The method was created based on procedures for the design and rehabilitation of damaged buildings, which contain engineering concepts based on the behavior of the structure. It was realized that more attention should be paid to damage control during design. This can only be achieved by introducing non-linear calculations into the methodology of seismic calculations. One of the most suitable approaches, on which the pushover analysis is based, is to combine the nonlinear static method of gradual pushing with the spectral response methodology [3]. With this analysis, the structure is exposed, in addition to the gravity load, to the lateral forces from the earthquake.

The pushover analysis aims to define the dependence of the displacement of the last floor or roof of the structure, the so-called control point, and the shear force in the foundation that causes the first yielding in the structure. The control point should be located at the highest level of the structure. When the strength of individual load-bearing elements reaches the stress value at the limit of large elongations, yielding occurs in those elements and so-

* Marijana Janićijević: Dositejeva 19, 36000 Kraljevo, Republic of Serbia and janicijevic.m@mfkv.kg.ac.rs

called plastic hinges are formed. Incremental lateral load is applied until the target displacement is reached and a nonlinear capacity curve is formed. It is assumed that the structure can make several such cycles and behave in a hysteretic manner [4]. To obtain the capacity curve, the analysis is applied up to the displacement control value, which is 150% of the target displacement value. This curve is usually determined to represent the first mode of the structure's response based on the assumption that the response to seismic action occurs primarily in the fundamental mode of vibration of the structure. Given that the building is a system with multiple degrees of freedom, the capacity curve of such a system (MDOF system) transforms into the capacity curve of an equivalent system with one degree of freedom (SDOF system), so that the capacity of the structure can be compared with the given seismic requirements [5].

By applying this method, it is possible to select places where potential plasticization of the system would occur, thus creating the conditions for the desired fracture mechanism to form on the system. In this way, the controlled development of nonlinear deformations prevents the system from reaching a state of complete collapse.

The assessment of the seismic performance of the structure in this work was carried out using the program for structural analysis SeismoStruct. This program is based on the finite element method and can use various non-linear modeling techniques. When calculating the behavior of spatial frames during the analysis with static and dynamic effects, the program analyzes the structural elements with the help of materially and geometrically nonlinear models. In this way, the program can calculate the response of the structure and its elements [6].

3. NUMERICAL EXAMPLE

3.1. Behaviour factor q

The capacity of structural systems to resist seismic forces in the nonlinear range generally allows them to be designed to resist seismic forces that are less than those corresponding to linear-elastic response.

To avoid an explicit inelastic structural analysis during design, the dissipative capacity of the structure is taken into account by applying an elastic analysis based on the response spectrum reduced concerning the elastic, so-called design spectrum. This reduction is achieved through the predominantly ductile behaviour of the structure and its elements, by introducing the behaviour factor q .

The behaviour factor q is an approximation of the ratio of seismic forces that the structure would experience if its response were fully elastic with 5% viscous damping and seismic forces that can be used in the elastic analysis while ensuring a satisfactory response of the structure. Its value defines the level of seismic load at the boundary between the elastic and plastic behaviour of the structure. The higher its value, the smaller the values on the design spectrum. Therefore, for lower values of the seismic load, the construction will move into the elastic area of operation. The value of the behaviour factor q can be different in different horizontal directions of the structure, while the ductility class is the same in all directions.

Upper limit value of the behaviour factor q shall be derived for each design direction as follows:

$$q = q_0 \cdot k_w \geq 1,50 \quad (1)$$

where:

q_0 is the basic value of the behaviour factor, depending on the type of the structural system and its regularity in elevation;

k_w is the factor reflecting the prevailing mode in structural systems with walls [7].

For buildings that are regular in elevation, the basic values of q_0 for the various structural types are given in Table 1.

Table 1. Basic value of the behaviour factor, q_0

STRUCTURAL TYPE	DCM	DCH
Frame system, dual system, coupled wall system	$3,0\alpha_u/\alpha_1$	$4,5\alpha_u/\alpha_1$
Uncoupled wall system	3,0	$4,0\alpha_u/\alpha_1$
Torsionally flexible system	2,0	3,0
Inverted pendulum system	1,5	2,0

α_1 and α_u are defined as follows:

α_1 is the value by which the horizontal seismic design action is multiplied to first reach the flexural resistance in any member in the structure, while all other design actions remain constant;

α_u is the value by which the horizontal seismic design action is multiplied, to form plastic hinges in a number of sections sufficient for the development of overall structural instability, while all other design actions remain constant [7].

Since the construction belongs to the group of constructions of the frame system and for the adopted ductility class DCH, the basic value of the behaviour factor is calculated as:

$$q_0 = 4,5 \cdot \frac{\alpha_u}{\alpha_1} \quad (2)$$

The value of α_u/α_1 is 1.3 for multi-storey, multi-bay frames, or frame-equivalent dual structures and factor k_w has a value of 1.

Total behaviour factor is:

$$q = q_0 \cdot k_w = 4.5 \cdot 1.3 \cdot 1 = 5.85 \quad (3)$$

3.2. Construction modeling

A five-storey reinforced concrete building was analyzed according to the recommendations in EN 1990, EN 1991, EN 1992-1, and EN 1998-1. The raster of the structure is shown in Figure 1. The length of a span in longitudinal and transverse directions is 5 m. The basic dimensions of the building are 15 x 25 m, and the height of the floors is constant at 2.8 m. The concrete material is C30/37 according to Eurocode 2, and the reinforcing steel is class B500B.



Figure 1. 3D model of the structure in SeismoStruct

During the analysis, the effects of seismic action and gravity (constant and variable) load were considered. Seismic impacts were determined by multimodal analysis with a design spectrum for the horizontal direction. To calculate the earthquake impact on the structure, an elastic response spectrum, type 1 (EN 1998) was used, for ground type C ($S=1.15$, $T_b=0.2s$, $T_c=0.6s$, and $T_d=2s$), with the reference peak ground acceleration which amounts $ag=0.2g$. Since the building has a business-residential function, it corresponds to the class of importance II, for which the value of the important factor is $\gamma=1$. The damping value is 5% and the correlation factor due to damping is $\eta=1$.

For the analyzed construction, a high ductility class DCH was adopted.

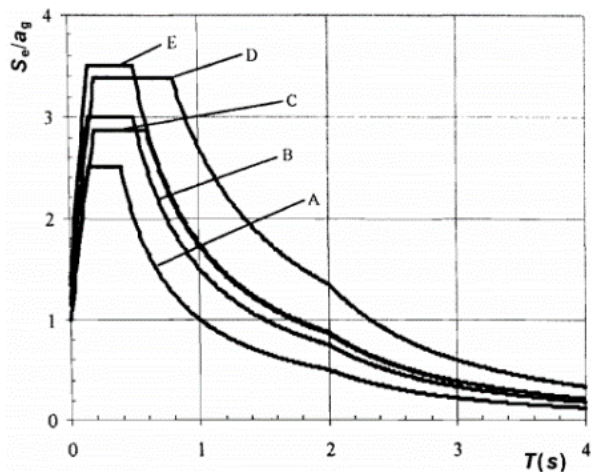


Figure 2. Recommended type 1 elastic response spectrum for soil categories A to E (5% damping)

The loads acting on the structure are as follows: permanent loads (G_i)- self-weight of the structural elements and an additional permanent load; the variable-live load (Q_i) and the seismic load (S_i). The assumed value of the permanent constant load is 6 kN/m² on all floors. The load intensity of the variable-live load is also 2 kN/m² on all floors. The value of the reduction factor of the variable-live loads is $\Psi_{2,i}=0.3$ (EN1990).

In T-section beams, the effective flange width, over which uniform conditions of stress can be assumed, depends on the web and flange dimensions, the type of loading, the span, the support conditions, and the transverse reinforcement [8]. The effective width of the flange should

be based on the distance l_0 between the points of zero moments, which may be obtained from Figure 3:

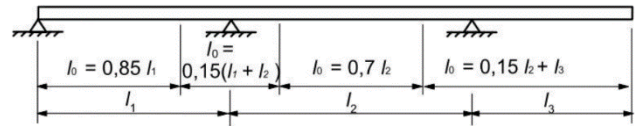


Figure 3. Definition of l_0 for calculation of effective flange width

The effective flange width b_{eff} for a T beam or L beam may be derived as [8]:

$$b_{eff} = \sum b_{eff,i} + b_w \leq b \quad (4)$$

with:

$$b_{eff,i} = 0,2 \cdot b_i + 0,1 \cdot l_0 \leq 0,2 \cdot l_0 \quad (5)$$

$$b_{eff,i} \leq b_i \quad (6)$$

(for the notations see Figure 3 above and Figure 4 below).

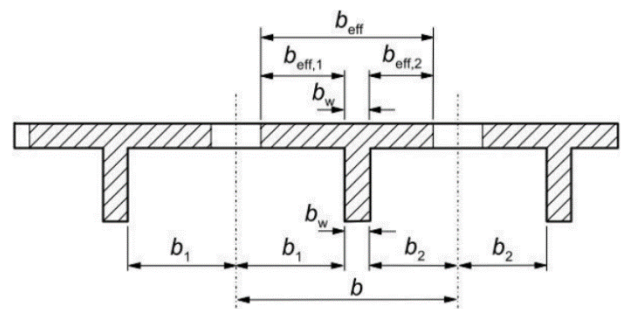


Figure 4. Effective flange width parameters

For structural analysis, where great accuracy is not required, a constant width may be assumed over the whole span. The value applicable to the span section should be adopted [8].

The dimensioning of the construction elements was carried out based on the authoritative combinations in the software package TOWER 8. The columns are square-shaped with dimensions of 0.45 x 0.45 m, and the beams are T and L cross-sections with dimensions: flange width 1.85 m, flange thickness 0.16 m, web width 0.45 m, and web height 0.19 m. The columns are reinforced with 12Ø28 and are weighted with stirrups UØ12/10cm on the length of the critical area and on the rest of the length UØ12/15cm. The beams at the support are reinforced in the upper zone with 5Ø20 and in the lower zone with 3Ø20, and the field in the lower zone with 3Ø20 and the upper zone with 2Ø20. Beam flanges are reinforced in the upper zone with Ø12/10cm and the lower zone with Ø12/20cm in both orthogonal directions. The cross-sections as well as the adopted layout of the element reinforcement are shown in Figure 5. The building meets the requirements of regularity in terms of base and height.

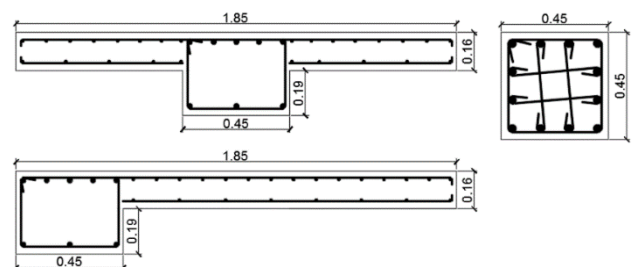


Figure 5. Cross sections of elements

The steel model used in the SeismoStruct is shown in Figure 6, and the concrete model is shown in Figure 7.

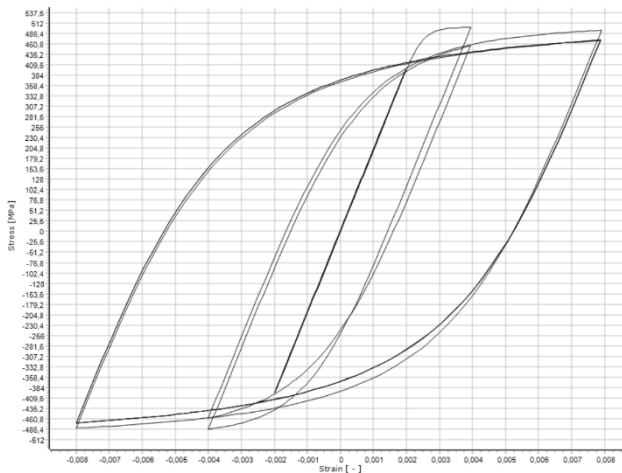


Figure 6. Uniaxial stress-strain relationship for steel reinforcement



Figure 7. Uniaxial stress-strain relationship for concrete

In critical sections, in addition to the load-bearing conditions, the conditions of local ductility are also met:

For beams:

reinforcement coefficient of the tensioned zone:

$$\rho = 0,7486 \% \leq \rho_{max} = 0,752 \%$$

compression zone reinforcement coefficient:

$$\rho' = 0,4489 \% \geq \rho_{tension} / 2$$

length of the critical zone:

$$l_{cr} = 1 \text{ m} \geq l_{cr,des} = 0,652 \text{ m}$$

For columns:

total reinforcement coefficient:

$$\rho_{min} = 0,01 \leq \rho = 0,0334 \leq \rho_{max} = 0,04$$

length of the critical zone:

$$l_{cl}/h_c = 2,45/0,45 = 5,44 > 3 \rightarrow l_{cr} = 0,675 \text{ m}$$

Fulfillment of requirements for adequate section weighting:

$$\alpha \cdot \omega_{wd} \geq 30 \cdot \mu_{\phi} \cdot v_d \cdot \varepsilon_{sy,d} \cdot \frac{b_c}{b_0} - 0,35 \rightarrow (0,333 > 0,2406)$$

After defining all the geometric and mechanical characteristics of the structure, a nonlinear static "pushover" analysis was carried out. The procedure was carried out for two orthogonal directions (X and Y) and the modal distribution of lateral forces.

Table 2. Forces in frame nodes for X and Y directions

Level	X	Y
V	183.366	122.244
IV	142.497	94.998
III	106.873	71.248
II	71.248	47.499
I	35.606	23.737

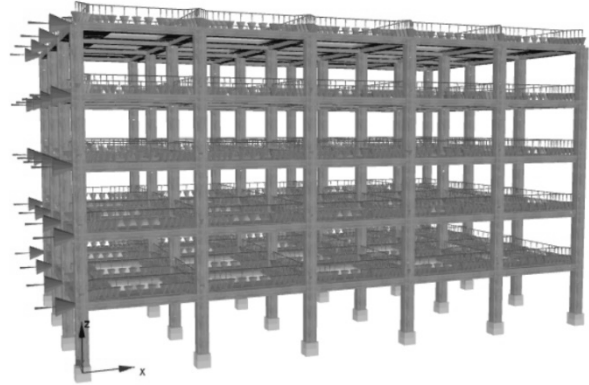


Figure 8. Applied loads in SeismoStruct for the X direction

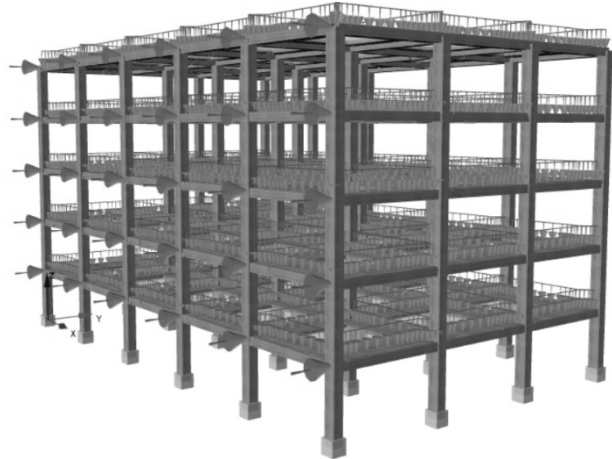


Figure 9. Applied loads in SeismoStruct for the Y direction

Four different models were created in the program for seismic analysis to show the different effects of material nonlinearity: inelastic frame element (*infrmFB* and *infrmDB*) and inelastic plastic-hinge frame element (*infrmFBPH* and *infrmDBPH*).

InfrmFB- The force-based model in SeismoStruct is a type of finite element model used to simulate the nonlinear behavior of structures under seismic loads. It is based on the force-based beam-column element approach, which considers the internal forces and deformations of each element in the structure [9].

In this model, each element of the structure is modeled as a series of the interconnected beam and column elements, which are connected at nodes. The internal forces and deformations of each element are calculated based on the axial force, bending moment, and shear force diagrams.

One of the advantages of the Force-based model is that it can accurately simulate the behavior of structures under different types of seismic loads, including ground motion and lateral forces. It can be used to evaluate the seismic performance of structures and to design retrofitting measures to improve their seismic behaviour [10].

In recent years, force-based models have been used extensively in conjunction with modern computational tools, such as finite element analysis and computer-aided design software, to optimize the seismic design of structures and to ensure their safety and performance during earthquakes.

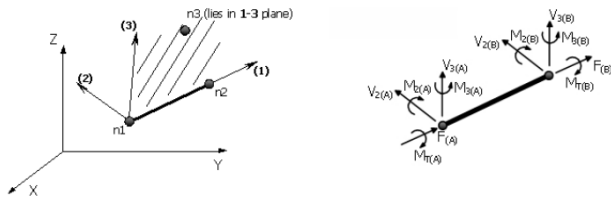


Figure 10. Local axes and output notation for elements [6]

InfrmDB- The displacement-based model in SeismoStruct is a type of finite element model used to simulate the nonlinear behavior of structures subjected to seismic loads. It is widely used in seismic analysis and design because it provides a more realistic representation of the actual behavior of structures under seismic loads. In this model, each element of the structure is divided into several smaller sub-elements, each of which is assumed to behave linearly elastically. The sub-elements are connected through nodes, and the displacement of each node is calculated based on the displacement of the neighboring nodes. The model also includes non-linear elements, such as plastic hinges, to represent the behavior of the structure beyond its elastic limit [11].

One of the advantages of the displacement-based model is that it is more accurate and reliable than the linear elastic model in predicting the response of structures under seismic loads. It can take into account the nonlinear behavior of the structure, such as the cracking and yielding of materials, and can provide more realistic estimates of the deformations and forces within the structure.

InfrmFBPH- The force-based plastic hinge model is a widely used modeling technique in the seismic analysis of structures. In this model, the plastic hinges are represented by two springs that act in parallel, one for the compression side and one for the tension side of the member [10]. The stiffness and strength of these springs are based on the yield strength and the cross-sectional properties of the member.

The model assumes that the member behaves in an elastic manner until the yield strength is reached, at which point plastic deformation occurs [12]. The plastic deformation is then accommodated entirely by the plastic hinge, while the rest of the member remains elastic. The plastic hinge is assumed to have a fixed length, which is defined by the user.

InfrmDBPH- In The Displacement-based plastic hinge model, the plastic hinges are represented by a non-linear element that is connected to the elastic members on either side of the hinge. The element has a specific displacement capacity, beyond which it undergoes plastic deformation. The element's displacement capacity is based on the yield strength and the cross-sectional properties of the member.

The displacement-based plastic hinge model assumes that the member behaves elastically until the displacement capacity of the plastic hinge is reached, at which point the plastic deformation occurs. The model accounts for the degradation of stiffness and strength of the

member after reaching the displacement capacity of the plastic hinge. The *infrmDBPH* element consists of 3 sub-elements, two joints at the edges of the member, which model plastic rotational deformations around the second and third local axes, and an elastic element in the middle, which models the part of the element that remains elastic [12].

A total of 8 "pushover" load cases are defined. For all 8 load cases, the increment method is controlled by displacements and a maximum displacement of 150% of the target displacement for the control point (master node), shown in Figure 11.

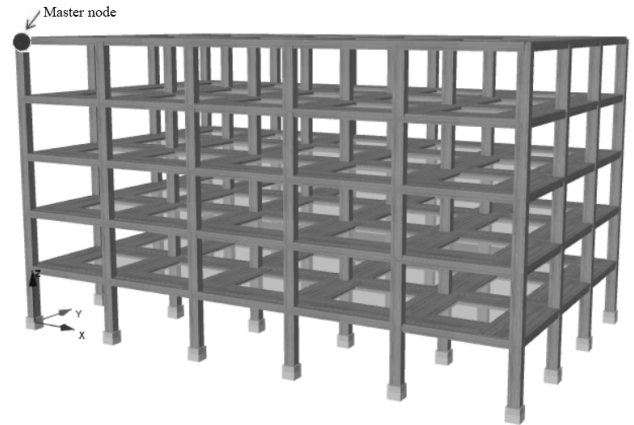


Figure 11. Master node

4. RESULTS

4.1. Target displacement

Target displacement is an important concept in seismic analysis, which refers to the expected amount of movement or deformation that a particular structure or component will experience during an earthquake or other seismic influence.

In general, the target displacement for a structure will depend on a variety of factors, including the expected severity and frequency of seismic events in the region, the type and size of the structure, and the materials used in its construction. By carefully analyzing these factors and designing structures to withstand the expected levels of displacement, engineers can help minimize the risk of damage and ensure the safety of people and property in areas prone to earthquakes.

Target displacement is defined as the seismic demand determined from the elastic response spectrum, through the displacement of the equivalent system with a single degree of freedom (SDOF) [citiraj dinamiku konstrukcija]. The mass of the equivalent SDOF system m^* is determined as:

$$m^* = \sum m_i \Phi_i = \sum \bar{F}_i \quad (7)$$

and the transformation factor is given by:

$$\Gamma = \frac{m^*}{\sum m_i \Phi_i} = \frac{\sum \bar{F}_i}{\sum \left(\frac{F_i^2}{m_i} \right)} \quad (8)$$

Force F^* and displacement d^* of the equivalent SDOF system is calculated as:

$$F^* = \frac{F_b}{\Gamma} \quad (9)$$

$$d^* = \frac{d_n}{\Gamma} \quad (10)$$

where F_b and d_n are based-shear and displacement, respectively, of the control node of the multi-degree of freedom (MDOF) system [7].

Yield force F_y^* , which also represents the limit bearing capacity of an idealized system, is equal to the base shear when a formation of the plastic mechanism occurs. The initial stiffness of the idealized system is defined so that the area under the actual and idealized force-displacement curve is equal. Based on this assumption, the yield displacement of the idealized SDOF system is given by:

$$d_y^* = 2 \left(d_m^* - \frac{E_m^*}{F_y^*} \right) \quad (11)$$

where E_m^* is the actual deformation energy up to the formation of the plastic mechanism (Figure 12)[7].

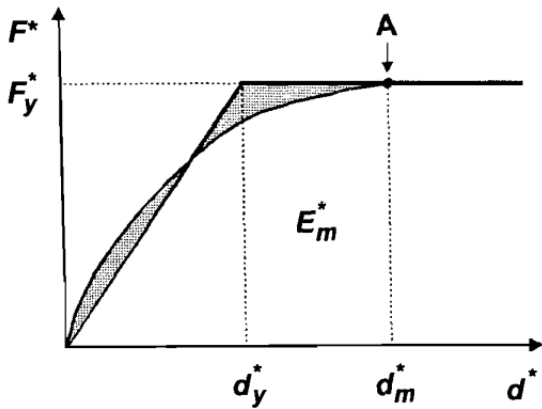


Figure 12. Idealized elastic-perfectly-plastic force displacement relation

Period T^* of the idealized equivalent SDOF system is determined by:

$$T^* = 2\pi \sqrt{\frac{m^* d_y^*}{F_y^*}} \quad (12)$$

Control displacement of the SDOF system for unlimited elastic behaviour equals:

$$d_{et}^* = S_e(T^*) \left[\frac{T^*}{2\pi} \right]^2 \quad (13)$$

where $S_e(T^*)$ is the acceleration obtained from the elastic response spectrum for the period T^* .

For $T^* < T_c$, target displacement is obtained from the following expressions:

$$\text{If } F_y^*/m^* \geq S_e(T^*), \text{ response is elastic:} \\ d_t^* = d_{et}^* \quad (14)$$

$$\text{If } F_y^*/m^* < S_e(T^*), \text{ response is inelastic:} \\ d_t^* = \frac{d_{et}^*}{q_u} \left(1 + (q_u - 1) \frac{T_c}{T^*} \right) \quad (15)$$

where q_u equals:

$$q_u = \frac{S_e(T^*) m^*}{F_y^*} \quad (16)$$

For $T^* \geq T_c$, target displacement is obtained from the expression (8), where d_t^* should not exceed the value $3d_{et}^*$.

Target displacement for the MDOF system is finally determined as:

$$d_t = \Gamma d_t^* \quad (17)$$

Based on the obtained calculation results, a very similar form of force-displacement dependence is noticeable, for both orthogonal directions. The highest value of the displacement of the master node when reaching 150% of the target displacement has the *infrmDBPH* model, and the least is the *infrmFB* model.

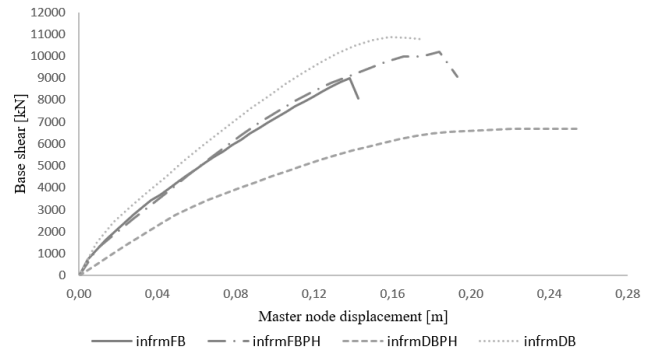


Figure 13. Pushover curves for X direction

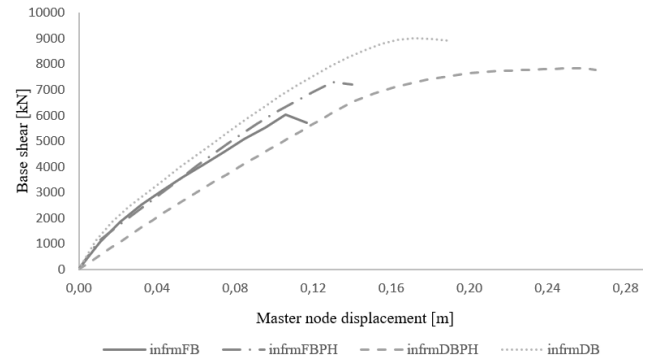


Figure 14. Pushover curves for Y direction

This is also very well visualized in Figure 15 plotting maximum base shear forces for all of the pushover load cases.

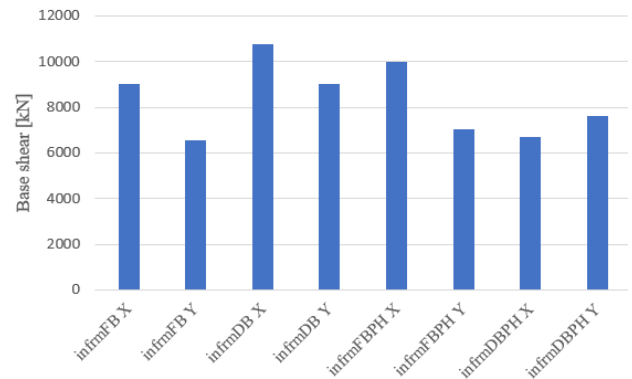


Figure 15. Maximum base shear vs. pushover load case

A manual verification of the results was performed. The calculation of the target displacement as well as the comparison with the results from the software is shown in Table 3 for the X direction and Table 4 for the Y direction.

Table 3. Calculation of target displacement for X direction

	infrmFB	infrmDB	infrmFBPH	infrmDBPH
Γ	1.063	1.063	1.063	1.063
F_y^*	9942.93	10856.61	10190.58	6693.19
d_m^*	0.23	0.153	0.1302	0.2378
E_m^*	888.81	395.66	448.66	623.58
d_y^*	0.281	0.233	0.172	0.289
T^*	0.751	0.654	0.580	0.928
$S_c(T^*)$	4.509	5.175	5.831	3.648
$d_t^* = d_{et}^*$	0.064	0.056	0.050	0.080
$d_t = \Gamma \cdot d_t^*$	0.068	0.060	0.053	0.085
SeismoStruct	0.067	0.060	0.059	0.083

Table 4. Calculation of target displacement for Y direction

	infrmFB	infrmDB	infrmFBPH	infrmDBPH
Γ	1.063	1.063	1.063	1.063
F_y^*	7652.32	9011.74	8126.6	7843.11
d_m^*	0.2338	0.172	0.13	0.2392
E_m^*	703.92	399.84	432.64	723
d_y^*	0.284	0.255	0.154	0.294
T^*	0.859	0.751	0.613	0.864
$S_c(T^*)$	3.939	4.506	5.517	3.917
$d_t^* = d_{et}^*$	0.074	0.064	0.053	0.074
$d_t = \Gamma \cdot d_t^*$	0.078	0.068	0.056	0.079
SeismoStruct	0.078	0.067	0.065	0.078

Relative floor displacement is shown in Figure 16 for the X direction and in Figure 17 for the Y direction. As shown in the Figures, model *infrmFBPH* has the lowest value of relative floor displacement.

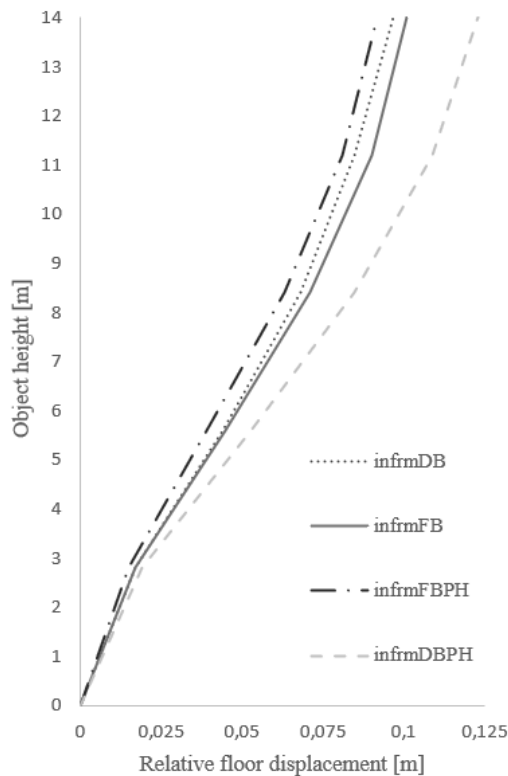


Figure 16. Relative floor displacement for X direction

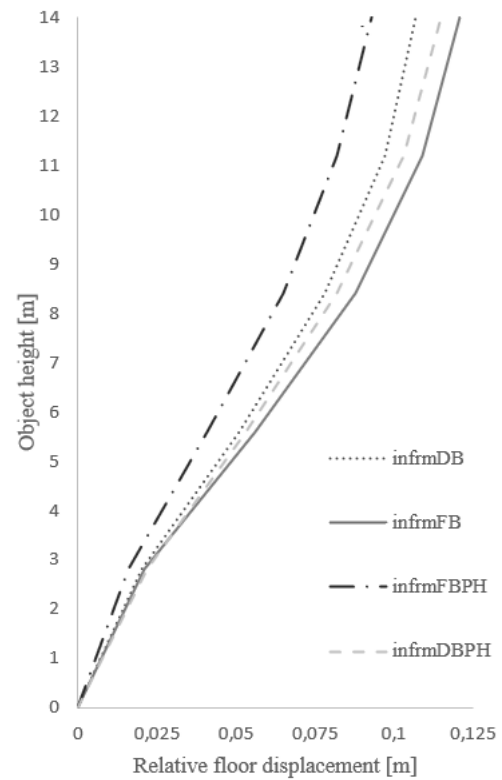


Figure 17. Relative floor displacement for Y direction

The schedule for the appearance of plastic hinges when reaching 150% of the target displacement is shown in Figure 18 and Figure 19. The considered criteria for the appearance of plastic hinges are shear capacity, yielding, concrete strain, fracture, and chord rotation. Figure 18 shows the schedule for the appearance of plastic hinges for the X direction and Figure 19 for the Y direction. As can be seen in the figures, plastic hinges occur when shear capacity and yielding conditions are exceeded.

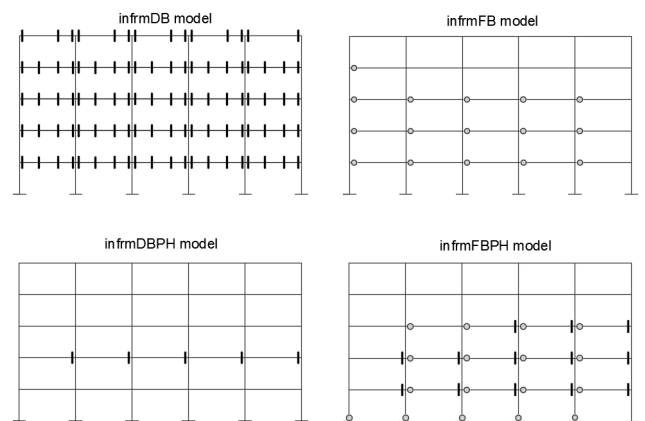


Figure 18. Schedule of appearance of plastic hinges for X direction (| -shear capacity; ● - yielding)

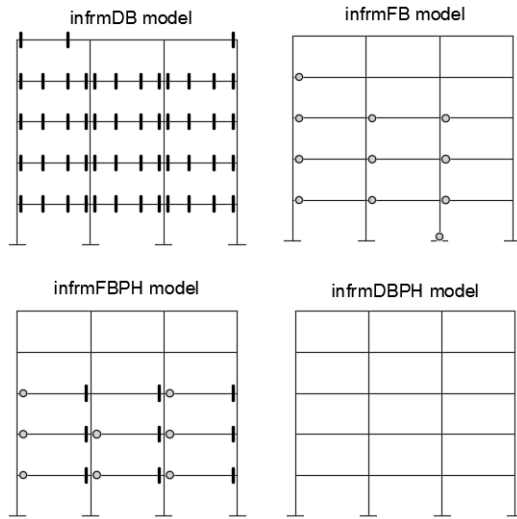


Figure 19. Schedule of appearance of plastic hinges for the Y direction (| -shear capacity; • - yielding)

Another criterion for evaluating the seismic performance of this building is the value of total chord rotation capacity. This value is calculated according to the expression 18 given in EN 1998-3:

$$\theta_{um} = \frac{1}{\gamma_{el}} \cdot 0.016 \cdot (0.3^v) \cdot \left[\frac{\max(0.01; \omega')}{\max(0.01; \omega)} \cdot f_c \right]^{0.225} \cdot \left(\frac{L_y}{h} \right)^{0.35} \cdot 25^{\left(\alpha \cdot \rho_{sx} \cdot \frac{f_{yw}}{f_c} \right)} \cdot (1.25^{100 \cdot \rho_d}) \quad (18)$$

where:

γ_{el} is equal to 1.5 for primary seismic elements and 1.0 for secondary seismic elements,

$v = N/bhf_c$ (b width of compression zone, N axial force positive for compression),

ω, ω' is the mechanical reinforcement ratio of the tension and compression, respectively, longitudinal reinforcement,

$L_v = M/V$ is the ratio moment/shear at the end section,

h is the depth of cross-section,

α is the confinement effectiveness factor,

$\rho_{sx} = A_{sx}/b_w s_h$ is the ratio of transverse steel parallel to the direction x of loading,

f_c and f_{yw} are the concrete compressive strength (MPa) and the stirrup yield strength (MPa),

ρ_d is the steel ratio of diagonal reinforcement (if any), in each diagonal direction [7].

Table 5 shows the results of the value obtained by applying expression 18, as well as their comparison with the limit values when reaching 150% of the target displacement.

Table 5. Values of total chord rotation for X and Y direction

	X direction		Y direction	
	demand	limit	demand	limit
infrmFB	0.0061	0.0683	0.0075	0.0744
infrmDB	0.0011	0.0409	0.0013	0.0436
infrmFBPH	0.0036	0.0693	0.0038	0.0811
infrmDBPH	0.0069	0.073	0.0089	0.721

5. CONCLUSION

Nonlinear static pushover analysis of a reinforced concrete building was performed using four different material nonlinearity models for two orthogonal directions. By observing the results of the seismic performance assessment of this object, the following conclusions are reached:

- pushover curves and target displacement: *infrmDBPH* model has the highest value of displacement (0.25 m for the X and 0.26 m for the Y direction); the *infrmFB* model has the lowest value of displacement (0.15 m for the X and 0.11 m for the Y direction);
- relative floor displacement: for the X direction, model *infrmDBPH* has the highest value (0.123 m) and the *infrmFBPH* model has the lowest value (0.092 m); for the Y direction, model *infrmFB* has the highest value (0.121 m) and *infrmFBPH* model has the lowest value (0.093 m);
- plastic hinges: due to exceeding the yield criteria, the models where plastic hinges appear are *infrmFB* and *infrmFBPH*; from the aspect of shear capacity criteria, the only model in which plastic hinges do not occur is *infrmFB* model;
- total chord rotation: the highest values have the *infrmDBPH* model (0.0069 for the X, and 0.0089 for the Y direction), and the lowest values have the *infrmDB* model (0.0011 for the X and 0.0013 for the Y direction).

Analyzing the results, it is concluded that the models with the mean values of the considered criteria (shear capacity, yielding, relative floor displacement, chord rotation capacity) are *infrmFB* and *infrmFBPH* models. Models *infrmDB* and *infrmDBPH* have extreme values of chord rotation and relative floor displacement.

REFERENCES

- [1] Lađinović, Đ.: Savremene metode seizmičke analize konstrukcija zgrada. Materijali i konstrukcije, 2008., vol. 51, № 1, p.p. 25-40.
- [2] Svilar, M., Prokić A.: Pushover analiza armiranobetonskog okvira. 7. međunarodna konferencija-savremena građevinska dostignuća u građevinarstvu 23-24.april 2019. Subotica, 2019., p.p. 363-370.
- [3] Obradović N., Mitković P., Radovanović S.: Nelinearna statička metoda postupnog guranja – pushover analiza AB okvira sa zidanom ispunom. Zbornik radova Međunarodnog simpozijuma o istraživanjima i primeni savremenih dostignuća u građevinarstvu u oblasti materijala i konstrukcija, Vršac, 18-20. oktobar 2017, 2017., pp. 245-254.
- [4] Petronijević M., Marjanović M., Radeka P.: Seismic Assessment of RC Buildings using N2 Method. Zbornik radova- Šesto međunarodno naučno-stručno savetovanje Zemljotresno inženjerstvo i inženjerska seizmologija, Beograd 13-15. jun 2018, 2018., pp. 387-395.
- [5] Radujković A., Rašeta A., Lađinović Đ.: Seizmička analiza AB okvirne konstrukcije primenom nelinearne metode N2, Zbornik Radova, DGKS, Simpozijum 2008, Zlatibor 2-26. septembar 2008, 2008. pp. 369-376.

- [6] SeismoStruct-User Manual, **2021**.
- [7] EN 1998-1, Design of structures for earthquake resistance - Part 1: General rules, seismic actions and rules for buildings, European Committee for Standardization. Brussels, **2004**.
- [8] EN 1992-1-1, Design of Concrete Structures, Part 1-1: General rules and rules for buildings, European Committee for Standardization. Brussels, **2004**.
- [9] Scott M. H., Fenves G. L.: Plastic Hinge Integration Methods for Force-Based Beam-Column Elements. Journal of structural engineering ASCE, **2006**. pp. 244-252.
- [10] Salehi M., Siders P., Liel A. B.: Seismic collapse analysis of RC framed structures using the gradient inelastic force-based element formulation. 16th World Conference on Earthquake, Santiago Chile 9-13. January 2017, **2017.**, vol. 12, № 2990.
- [11] Tarquini D., Almeida J. P., Beyer K.: An enhanced displacement-based element to account for tension shift effects. 16th World Conference on Earthquake, Santiago Chile 9-13. January 2017, **2017.**, vol. 12, № 3167.
- [12] Rajić N., Lađinović Đ.: Nonlinear static seismic analysis of multi-story RC building, *6. međunarodna konferencija-savremena građevinska dostignuća u građevinarstvu 21.april 2017. Subotica*, **2017.**, p.p. 287-295.